# Experimental and theoretical studies of the thermal degradation of a phenolic dibenzodioxocin lignin model

**ARTICLE** *in* WOOD SCIENCE AND TECHNOLOGY · JANUARY 2012

Impact Factor: 1.92 · DOI: 10.1007/s00226-012-0478-7

# *Experimental and theoretical studies of the thermal degradation of a phenolic dibenzodioxocin lignin model*

**Christian Gardrat, Reinaldo Ruggiero, Marie-Thérèse Rayez, Jean-Claude Rayez & Alain Castellan**

**Wood Science and Technology**
Journal of the International Academy of Wood Science

ISSN 0043-7719
Volume 47
Number 1

Wood Sci Technol (2013) 47:27-41
DOI 10.1007/s00226-012-0478-7


Springer

Wood Sci Technol (2013) 47:27–41
DOI 10.1007/s00226-012-0478-7

ORIGINAL

# Experimental and theoretical studies of the thermal degradation of a phenolic dibenzodioxocin lignin model

**Christian Gardrat · Reinaldo Ruggiero · Marie-Thérèse Rayez · Jean-Claude Rayez · Alain Castellan**

Received: 17 March 2011 / Published online: 30 March 2012


**Abstract** A large part of biphenyl structures in lignin are etherified by α- and β-carbons of another phenylpropane unit to give an eight-member ring called dibenzodioxocin. The behavior of a phenolic dibenzodioxocin lignin model, 4-(4,9-dimethoxy-2,11-*n*-dipropyl-6,7-dihydro-5,8-dioxa-dibenzo[a,c]cycloocten-6-yl)-2-methoxyphenol (DBDOH, **1**), was studied by different mass spectrometry and thermal methods, leading to the conclusion that dibenzodioxocins are thermally unstable products. Both semi-empirical and density functional theory quantum calculations show that both C–O bonds, which connect the biphenyl part of the dibenzodioxocin molecule to the phenolic group, can be broken under increasing temperature. However, they do not play the same role since their dissociation occurs through different barrier heights. The C–O bond directly connected to the phenolic group (α–O-4) will dissociate first since its barrier energy for scission is lower than the other one (β–O-4), by roughly 12 kcal $mol^{-1}$ ($\approx$50 kJ $mol^{-1}$). This conclusion is likely applicable to thermal degradation of DBDO units in lignin polymer.

C. Gardrat · A. Castellan (✉)
Laboratoire de Chimie des Polymères Organiques, IPB/ENSCBP, Université Bordeaux 1, 16 avenue Pey-Berland, 33607 Pessac Cedex, France
e-mail: acastellan@ipb.fr

C. Gardrat · A. Castellan
Laboratoire de Chimie des Polymères Organiques, Centre National de la Recherche Scientifique, 33607 Pessac cedex, France

R. Ruggiero
Laboratorio de Fotoquímica e Materiais Lignocelulósicos, Universidade Federal de Uberlândia, P.O. Box. 596, Uberlândia, Brazil

M.-T. Rayez · J.-C. Rayez
Institut des Sciences Moléculaires, Université Bordeaux 1, UMR 5255, 33405 Talence Cedex, France

## Introduction

Dibenzodioxocins (DBDO) are a class of wood components recently discovered in lignin, mainly in softwood, where a large part of 5-5′-biphenyl structures are etherified as eight-member rings including both α- and β-aryl ether bonds (Karhunen et al. 1995a, b, 1996). They constitute a large part of the polymer network and are considered as the most important branching structures in lignins (Karhunen et al. 1995a, b; Argyropoulos et al. 2002; Kukkola et al. 2003). The influence of DBDO's was studied in chemical pulping and bleaching (Akim et al. 2001; Argyropoulos 2003). In particular, the behavior of some model compounds under soda and kraft pulping conditions have been examined (Karhunen et al. 1999). The photochemical and photophysical reactivities of a few synthesized models of dibenzodioxocins have already been described (Gardrat et al. 2004, 2005; Machado et al. 2006). A new concise approach of the synthesis of dibenzodioxocin subunit has also been proposed (Zawisza et al. 2006). Recently, some phenolic and amine derivatives were enzymatically grafted to DBDO using fungal laccases (Kudanga et al. 2010).

The thermal stability of DBDO's has never been examined, whereas pyrolysis reactions of lignin models have been considered (Elder 2010). To the authors' knowledge, there is only one study dealing with delignification mechanisms during high boiling solvent pulping (temperature higher than 200 °C) where the authors suggested that the dibenzodioxocins were not stable under their pulping conditions and were cleaved even without the presence of acids (Kishimoto and Sano 2003; Kishimoto et al. 2004).

In this study, it is intended to demonstrate that a model of phenolic DBDO is thermally unstable using different mass spectrometry and thermal methods. In order to determine the most sensitive bonds of the dioxocin ring able to break, quantum chemical calculations were performed at different levels of theory: semi-empirical AM1, density functional theory (DFT) with B3LYP and M062X functionals.

## Experimental

### Materials

The dibenzodioxocin model, 4-(4,9-dimethoxy-2,11-*n*-dipropyl-6,7-dihydro-5,8-dioxa-dibenzo[a,c]cycloocten-6-yl)-2-methoxyphenol, DBDOH, **1** was prepared, as already described (Gardrat et al. 2004). MBTFA (N-methyl-bis-trifluoroacetamide) was purchased from Sigma-Aldrich (France) and used to protect phenolic functions as follows: the phenolic substance (about 1 mg), MBTFA (20–80 μL) and pyridine (20–100 μL) were introduced in a vial and heated to the desired temperature (60–80 °C) for 20–120 min. GC analysis was performed after cooling to room temperature.

## Mass spectrometry analyses

Low-resolution electron ionization (EI-MS) mass spectrum (EI 70 eV) of DBDOH, **1** was registered after direct introduction via a heating probe using a VG Micromass AutoSpec Q (Micromass UK, Manchester, England) spectrometer. Gas chromatography (GC)/EI-MS analyses were performed with a Finnigan Trace (ThermoFisher Scientific, Courtaboeuf, France) mass spectrometer (electron energy 70 eV) interfaced with a Finnigan Trace GC Ultra gas (ThermoFisher Scientific, Courtaboeuf, France) apparatus (transfer line temperature : 250 °C) equipped with a programmed temperature vaporizer (PTV) injector (splitless mode) using helium as carrier gas. Three phases were programmed for the PTV injector: injection at 30 kPa, 0.20 min; transfer at 30 kPa, temperature from 40 to 300 °C at a rate of 10 °C $s^{-1}$ followed by a cleaning step. A fused silica capillary column (RTX-5MS, 15 m, 0.25 mm i.d., film thickness 0.25 μm) was selected. The oven temperature was programmed from 40 °C (initial hold time of 1 min) to 320 °C at a rate of 15 °C $min^{-1}$; this final temperature was maintained for 15 min. When using MBTFA, a solvent delay of 5 min was sufficient to remove most of the derivatization products from the column.

Pyrolyses were performed at different temperatures with a Pyrojector II SGE (Interchim, Montluçon, France) coupled to a Varian Saturn 4D GC–MS (Varian SA, Les Ulis, France) using a 30 m × 0.25 mm RTX-20 column (film thickness 1 μm) in split mode. The oven was programmed from 40 °C (2 min) to 280 °C at a rate of 15 °C $min^{-1}$. The final temperature was held for 30 min. The injector temperature was kept at 200 °C.

The different structures reported in this paper were proposed after comparison of their mass spectra with those reported in literature or in the NIST library and after interpretation of the main peaks (Mc Lafferty and Turecek 1993). In all chromatograms, amounts of the products were calculated as a direct percentage of the peak areas (±10 %).

## NMR spectra

$^1$H NMR spectra were recorded on a Bruker DPX-300 (Wissembourg, France) using 15 mg of sample in 0.5 mL of $CDCl_3$ in a 5-mm tube.

## Thermal analyses

Thermogravimetry (TG) measurements were carried out with a Shimadzu DTG-60 H instrument (Shimadzu Do Brasil, Comercio LTDA, São Paulo, SP, Brazil) on 5.4 mg of DBDOH sample weighed on a platinum pan and heated from 22 to 700 °C at 10 °C $min^{-1}$ under nitrogen flow rate (30 mL $min^{-1}$). The results were also analyzed by the first derivative (DTG). Differential Scanning Calorimetry (DSC) analysis was carried out with a Q-20 TA Instrument (TA Instruments, Jabaquara-São Paulo, SP, Brazil) from approximately 5.4 mg of DBOH sample (deposited on an aluminum pan) under nitrogen flow rate of 30 mL $min^{-1}$ and heating rate of 10 °C $min^{-1}$. The sample was heated from 25 to 500 °C.

## Theoretical methodology

In order to give arguments to support the experimental work, the cleavage propensity of two bonds involving the same kind of atoms (C and O) in the same structure only differentiated by the presence of a substituent needs to be compared. Therefore, the use of a semi-empirical approach is fully justified for good reasons (easiness of use even for large systems, realistic and reliable description of chemical behavior for C/H/O systems). AM1 parameterization was selected, which was proposed in the 80s by Dewar et al., and has already proved its efficiency to describe the structures including C/H/O atoms and especially hydrogen bonding. AM1 is well known to be a reliable tool to provide useful information to experimentalists. The semi-empirical calculations were performed using the AMPAC 9 package (AMPAC$^{TM}$ 1992–2008), which also contains all the references to the methodology, at different levels of calculations: Unrestricted Hartree–Fock (UHF), Half-Electron Hartree–Fock (HEHF) and Configuration Interaction with Single, Double excitations (CISD) based on the HEHF previous description.

The geometries of the minima and saddle points (or cols) involved in the decomposition reactions were fully optimized. The saddle points are characterized by the existence of only one negative eigenvalue of the Hessian matrix corresponding to an imaginary frequency in the normal mode analysis. The transition states were considered to be located at the saddle points along the reaction paths. Their connection was checked with the corresponding minima using the intrinsic reaction coordinate (IRC) approach as implemented in the AMPAC 9 package. In order to check whether the results were independent of the method, the density functional theory B3LYP (Becke 1993) as well as the more recent M06-2X theory, proposed by Truhlar parametrized to give reliable thermochemical kinetics (Zhao and Truhlar 2008), were employed. Both methods were used at the UHF level and with the 6-31G(d,p) basis set. The Gaussian09 program (Gaussian and Revision 2009) was used for these calculations.

## Results and discussion

### Direct introduction/EI-MS

In the low-resolution mass spectrum of DBDOH, **1** many ions are seen (Fig. 1). An interpretation has already been proposed for some of them (Gardrat et al. 2005). Nevertheless, the presence of the ion at m/z 150 is unexpected. A series of ions at m/z 135 (loss of 15 Da) and m/z 107 (loss of 28 Da from m/z 135, likely carbon monoxide) are also observed. The relative abundance of the peak at m/z 150 depends on the heating rate of the probe: 10 % at 50 °C min$^{-1}$ (Fig. 1a) and 21 % at 80 °C min$^{-1}$ (Fig. 1b), whereas other peaks are practically unchanged. As the molecular ion ($M^{+\cdot}$ 478) is also the base peak, it can be concluded that this ion is very stable (Mc Lafferty and Turecek 1993) and that the relative abundance of the ion at m/z 150, depending only on the heating rate of the probe, is likely due to a thermal degradation of **1**. Thus, this peak does not belong to a fragment of $M^{+\cdot}$. The

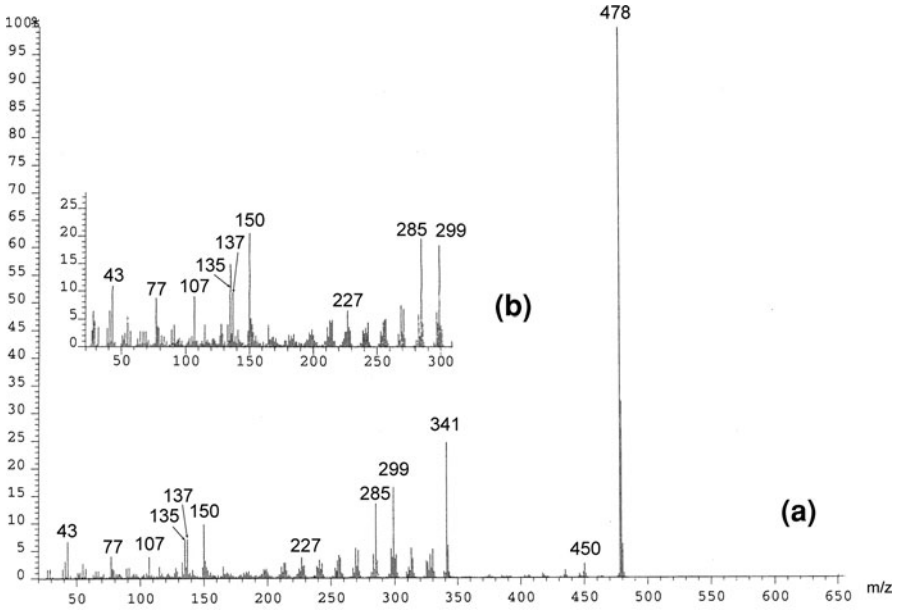


**Fig. 1** **a** Low-resolution mass spectrum of DBDOH, **1** with a heating rate of the probe fixed at 50 °C $min^{-1}$; **b** zoom of the 0–300 mass units region of the low resolution mass spectrum with a heating rate of the probe fixed at 80 °C $min^{-1}$

spectrum of the degradation product can be attributed with a large confidence level to 4-vinylguaiacol **2**.

## GC/EI-MS analyses

The total ion chromatogram (TIC) of DBDOH, **1** in acetone solution is represented in Fig. 2. The mass spectra of the different diastereoisomers ($M^{+\cdot}$ 478, retention times at 19.75 and 20.28 min) are practically identical. Therefore, the attribution of the different structures is quite impossible. It should be noted that no ions at m/z 150 do appear in the spectra, in accordance with the preceding interpretation. Besides the dibenzodioxocin **1** peaks, two other ones are observed in the TIC spectrum: the former with the smaller retention time (6.54 min) can easily be attributed to 4-vinylguaiacol **2** ($M^{+\cdot}$ 150) and the latter at higher retention time (16.01 min) corresponds to 3,3′-dimethoxy-5,5′-dipropyl-biphenyl-2,2′-diol **3** ($M^{+\cdot}$ 330), which is used in the synthesis of **1**. The comparison of $^{1}H$ NMR spectra of neat samples of **1, 2** and **3** (Fig. 3) proves that the synthezized DBDOH, **1** is a pure compound.

The replacement of hydroxyl groups by trifluoromethylacetoxyl ones allows the preparation of more volatile products. A reaction of **1** and **3** with MBTFA was undertaken. For compound **3**, the reaction is complete at 80 °C after 1 h, and a single peak is obtained by GC/MS ($M^{+\cdot}$ 522; compound **3-F**) with a dramatic diminution of the retention time (13.01 min *vs* 16.01 min). For compound **1**, the esterification does not occur completely; there always remains unprotected

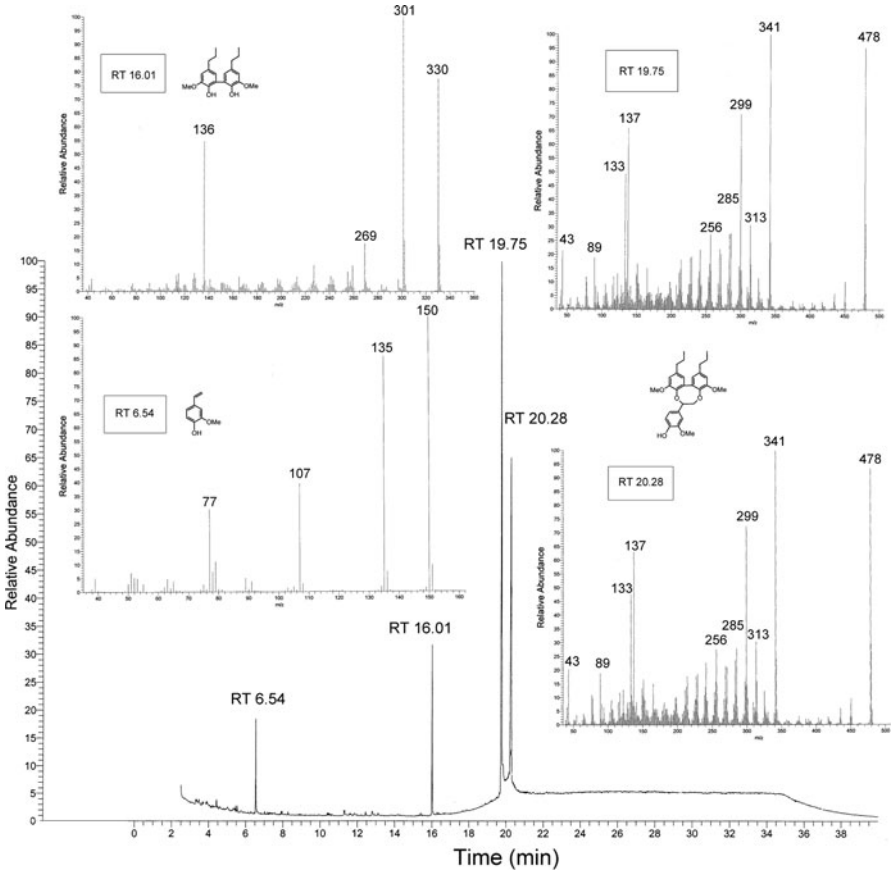


**Fig. 2** Total ion chromatogram (TIC) of DBDOH in acetone

DBDOH, **1**, but its amount depends on the experimental conditions. Maybe some steric hindrance limits the reaction, as it was reported on the derivatization of other phenols by silylating reagents (Schummer et al. 2009). Relative areas of the peaks (GC–MS analysis) observed for all the compounds after different experimental conditions for silylation of DBDOH are given in Table 1. By contrast with compound **3**, the retention times of the main peaks for protected DBDOH ($M^{+\cdot}$ 574; compound **1-F**) compared with the unprotected one are only slightly diminished (19 vs. 20 min).

As the degree of protection of compound **1** increases, the presence of **2** and **3** decreases, but the ratio remains practically constant. The potential presence of protected **2** was not evidenced due to the conditions of the GC/MS coupling. All these observations seem to indicate that **2** and **3** are formed from compound **1** during the GC analysis, likely during the injection procedure.

Another interesting proof of the thermal instability of compound **1** was obtained in studying the photodegradation products formed after 3-h irradiation with medium-pressure mercury lamps (400 W) at room temperature in non-degassed


**Fig. 3** $^{1}$H NMR spectra of compounds **1**, **2** and **3**

**Table 1** Protection of DBDOH, **1** with MBTFA under different experimental conditions; Peak area percentages of the different compounds given by GC–MS analysis

| MBTFA (μL) | Pyridine (μL) | T (°C) | Duration (min) | Products (direct area percentages) | | | |
|---|---|---|---|---|---|---|---|
| | | | | **2** | **3** | **1-F** | **1** |
| 30 | 40 | 70 | 35 | 34 | 21 | 18 | 27 |
| 30 | 40 | 70 | 60 | 29 | 18 | 33 | 20 |
| 80 | 100 | 80 | 120 | 15 | 9 | 61 | 15 |

ethanol (Gardrat et al. 2005). In this study, it was observed that, after derivatization with MBTFA, the TIC displayed a lot of peaks (Fig. 4).

Among them, the peaks corresponding to unreacted unprotected DBDOH, **1**, unreacted protected DBDOH, **1-F**, unprotected **3**, protected **3** (**3-F**), and unprotected

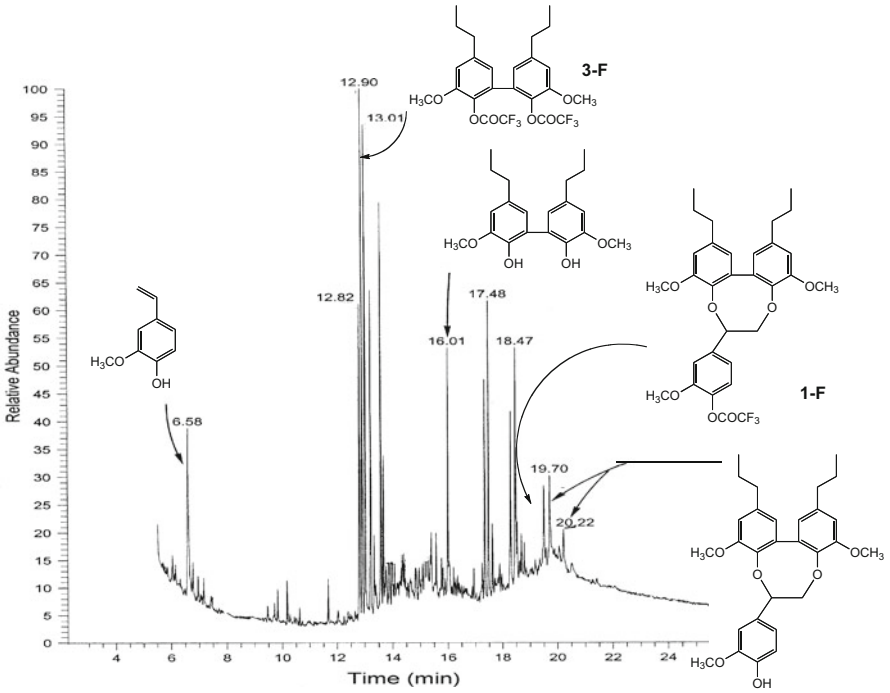


**Fig. 4** TIC of photolysis products of DBDOH, **1** after treatment by MBTFA

**2**, were detected. According to this observation, it is likely that compound **3** was obtained by two different pathways: photodegradation leading to **3-F** after derivatization and thermal degradation giving unprotected compound **3**.

## Pyrolysis/GC/EI-MS analyses

Dibenzodioxocin **1** was submitted to pyrolysis at three different temperatures: 200, 300, and 400 °C. Different products of thermal degradation were separated by gas chromatography using a capillary column with a thick film and identified by EI-MS. The presence of carbon dioxide was detected at temperatures higher than 300 °C. The relative areas of the compounds given by GC–MS analysis are presented in Table 2.

**Table 2** Analysis by GC–MS of the degradation products after pyrolysis of DBDOH, **1**

| Pyrolysis temperature (°C) | Compounds (direct area percentages) | | | | | | |
|---|---|---|---|---|---|---|---|
| | **2** | **4** | **5** | **6** | **7** | **8** | Not identified |
| 200 | 100.0 | – | – | – | – | – | – |
| 300 | 95.1 | 2.4 | 0.6 | 0.4 | 0.7 | 0.6 | 0.2 |
| 400 | 90.3 | 3.1 | 1.1 | 1.1 | 2.1 | 0.8 | 1.5 |

In all cases, 4-vinylguaicol **2** is the main observed degradation product. It is noticeable that, even at relatively low temperature, the dibenzodioxocin is thermally unstable. As the pyrolysis temperature increases, other products are formed: the propyl side chain was split off completely (compound **4**), shortened to one (compound **5**) or two (compound **6**) carbons or fully conserved (compound **7**). New double bonds are also created in the side chains through pyrolytic dehydrogenation (compound **8** appears as its two Z/E isomers). It is likely that compound **3** was not detected due to the analytical conditions used, especially the large film thickness of the GC column. For this reason, the pyrolysis of compound **3** was studied at 400 °C. The main degradation products were **5** (0.6 %), **6** (3.5 %), **7** (69.6 %), and **8** (26.0 %), corresponding to the cleavage between the two phenyl groups (**7**), splitting (**5**, **6**) and dehydrogenation (**8**) of the side chain. Similar observations have already been reported by Domburg et al. (1970) with dehydrodivanillin. Domburg et al. (1970) concluded that biphenyl bond degradation takes place according to a free radical mechanism; moreover, they established that under thermal treatment, the methoxy groups did not split off. It should be also noted that no degradation products were formed even at 400 °C in a structure with a 5,5′-linkage looking like **3**, but with methyl groups instead of propyl ones (Kawamoto et al. 2007; Nakamura et al. 2008).

## Thermal properties of DBDOH, **1**

In order to complete the mass spectrometry studies, TG, DTG (Fig. 5), and DSC (Fig. 6) measurements on DBDOH were also performed. Figure 5 indicates that DBDOH is highly decomposed from 240 °C and completely destroyed at 600 °C. Figure 6 shows that this process is mainly an exothermic one with exothermic peaks at 234 and 433 and endothermic peaks at 330, 354, and 420 °C. In addition, an endothermic peak is observed at 154 °C (Fig. 6) and at 153 °C (Fig. 5) in the DTG curve. These peaks are likely due to the liberation of some vinylguaiacol already seen by pyrolysis/mass spectrometry. The lack of important mass loss observed in

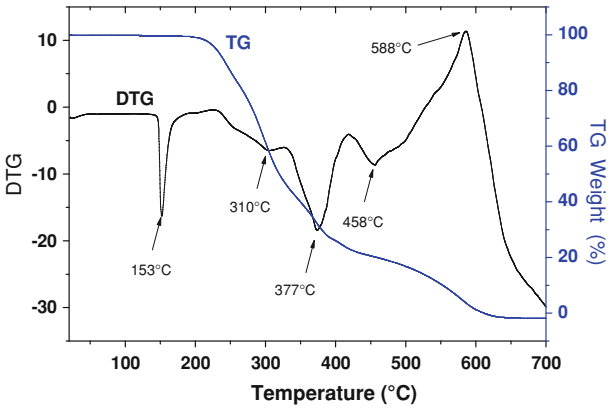


**Fig. 5** TG and DTG analyses of DBDOH, **1** (Nitrogen flow rate: 30 mL $min^{-1}$)

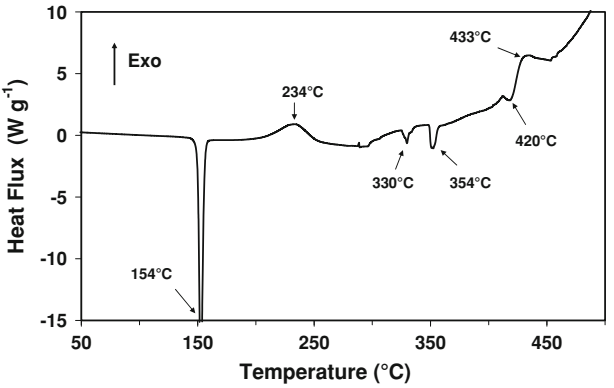


**Fig. 6** DSC analysis of DBDOH, **1** (Nitrogen flow rate: 30 mL $min^{-1}$)

the TG curve might be due to some trapping by the matrix of this very reactive structure including both phenol and styrene elements.

## Thermal degradation pathways of dibenzodioxocin **1**

All the preceding results show that dibenzodioxocin **1** is thermally unstable even at relatively low temperatures. This product is decomposed in 4-vinylguaiacol **2** and in

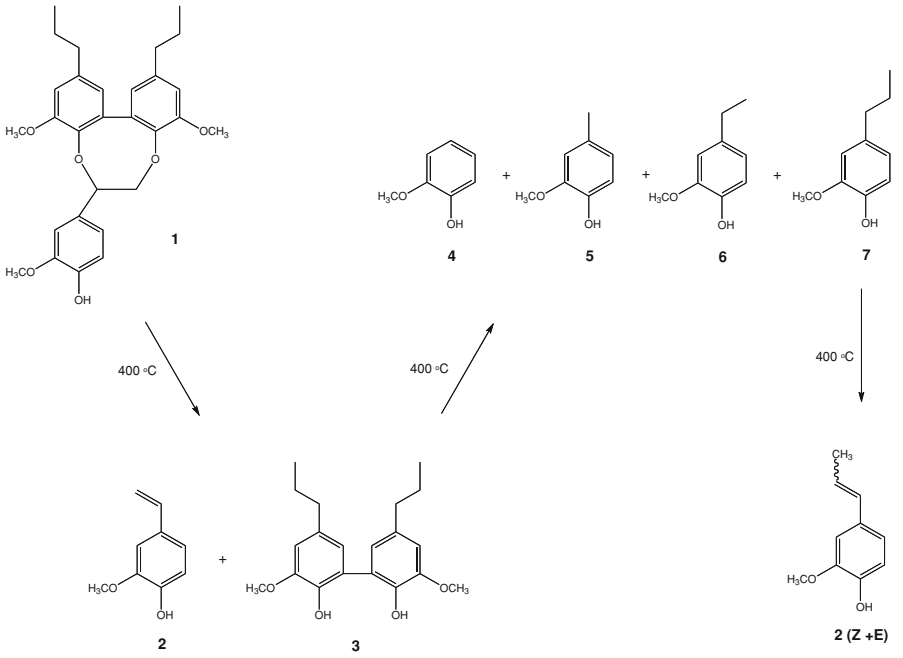


**Fig. 7** Thermal degradation of dibenzodioxocin **1** at 400 °C

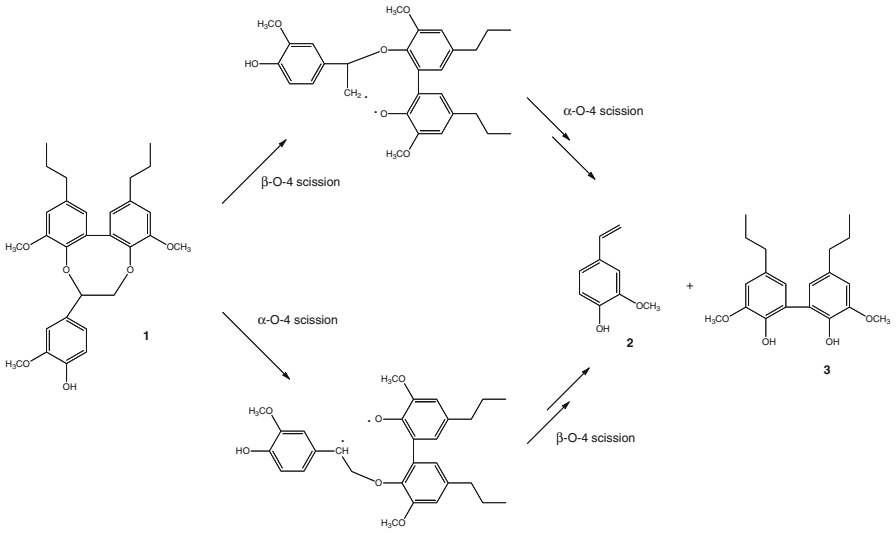


**Fig. 8** Thermal degradation possibilities of compound **1**

the diphenolic compound **3**, which is then thermally degraded at higher temperatures according to Fig. 7.

The formation of 4-vinylguaicol **2** from pyrolysis of DBDOH, **1** can be accounted by two mechanisms: either an α–O-4 scission followed by a *β*–O-4 one or the contrary (Fig. 8).

In the past, it was assumed that the reactivity of the molecular ion obtained in EI-MS could be used to directly deduce the reactivity of the same molecule in photochemical or thermochemical processes. In fact, parallels were found between pyrolysis reactions, photochemistry, and electron-impact mass spectrometry, but it seems that the relationships, when they occur, are only coincidental (Dougherty 1974). Fragmentation pathways in EI-MS are driven by the properties of a radical-cation species, whereas in pyrolysis they are driven by cleavage of the weakest bond in the precursor molecule. A good example was given by Black et al. (1994).

Photochemical studies combined with a theoretical approach on phenolic and non-phenolic dibenzodioxocins (Gardrat et al. 2004, 2005; Machado et al. 2006) suggested that photooxidation of dibenzodioxocins is a complex mechanism involving a two-step homolytic bond cleavage (α–O-4 and then *β*–O-4). Moreover, the formation of the main fragmentation peak at m/z 341 (relative abundance 24 %) in the mass spectrum of **1** (EI-MS, 70 eV) was explained (Gardrat et al. 2005) by a primary cleavage of the C–C bond of the dioxocin ring and elimination of a 4-guaiacylmethyl radical.

## Quantum calculations

In order to put some light on the mechanism of the formation of **2**, it was decided to perform quantum calculations on a DBDO model, **1-M** (stereoisomer (a) in Fig. 9) a

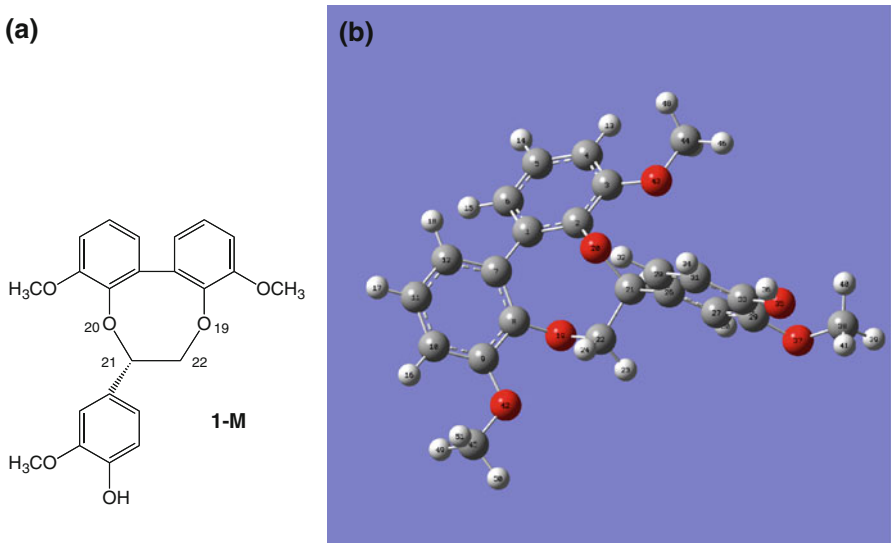


**Fig. 9** **a** Formulae of DBDO model **1-M** used for calculations **b** Representation of DBDO model **1-M** used for calculations. The C–O bonds concerned in the study are the bonds 20–21 (α–O-4) and 19-22 (*β*–O-4)

little bit simpler than the true molecule since the two propyl chains linked to the biphenyl skeleton are replaced by hydrogen atoms. This simplification is justified by the fact that these two alkyl tails do not play a significant role in the mechanism investigated in this work. The purpose of this theoretical study is to analyze which of the two C–O bonds α–O-4 or *β*–O-4, both connecting the biphenyl structure to the phenolic one, is the most easily breakable (see Fig. 8). Using the methodologies defined in the theoretical section, a barrier (transition state, TS) was located along the reaction path for dissociation of each C–O bond for which the structure and energy was determined. It is worthwhile to note that, due to the presence of barrier heights, the problem is a kinetic one rather than a thermodynamic one which only involves bond strength without any information about its propensity to be broken (Table 3).

**Table 3** Energy height of the transition states (TS) with respect to the energy of the DBDO model molecule **1-M**

| Bond scission | UHF | HEHF (75–76)[c] | CISD (73–78)[d] |
|---|---|---|---|
| α–O-4 | 29.5[a] (1.98 Å)[b] | 45.4[a] (2.15 Å)[b] | 47.7[a] (2.25 Å)[b] |
| *β*–O-4 | 42.7[a] (2.13 Å)[b] | 53.5[a] (2.33 Å)[b] | 56.3[a] (2.33 Å)[b] |

[a] The barrier heights are expressed in kcal $mol^{-1}$

[b] The numbers in brackets are the values of the C–O bond distance at the TS

[c] The HEHF indices (75–76) give the label of the two molecular orbitals (MO) containing each two half electrons

[d] The CISD indices (73–78) are the labels of the MO involved in the single and double excitations

**Table 4** Energy height of the transition states (TS) with respect to the energy of the DBDO model molecule **1-M** using DFT-UB3LYP/6-31G(d,p) and DFT-UM062X/6-31G(d,p)

| Bond scission | UB3LYP | UM06-2X |
|---|---|---|
| α–O-4 | 27.4 | 35.8 |
| *β*–O-4 | 39.6 | 49.0 |

The barrier heights are expressed in kcal $mol^{-1}$

First the results from AM1-type calculations were analyzed. It is interesting to note that the UHF approach leads to lower barriers than the two other ones. This fact is not surprising since (1) UHF favors spin multiplicity mixing along the reaction path and (2) an UHF approach involves the double number of optimizing coefficients than any RHF like calculation. As a matter of fact, as long as the two C–O bonds are extended, the UHF wavefunction is no longer an eigenfunction of the square of the total spin angular momentum $S^2$ of the system. Fortunately, since the variation of the quantum average value of $S^2$ for both reaction paths is the same, the comparison of the energy variation along these two paths can be accepted with some confidence. Concerning now the HEHF and the CISD methods, the active space used (2 and 6 active molecular orbitals for HEHF and CISD, respectively) stabilizes more efficiently the closed shell electronic structure of **1-M** (minimum) than the open shell biradical structure of the two TSs. Such a situation leads to larger energy barriers than those calculated at the UHF level. Moreover, this CISD calculation stabilizes more efficiently the structure of the minimum than the HEHF one. This is why the energy barriers are larger with CISD than with HEHF, but the differences are small. Concerning now the DFT calculations, the energy barriers are collected in Table 4. Similar ordering is observed between the barrier heights of the two bonds which can undergo dissociation. Both tables show that, whatever the method used, the α–O-4 bond scission is favored by roughly 12 kcal $mol^{-1}$ ($\approx$50 kJ $mol^{-1}$) with respect to the *β*–O-4 one. Calculations performed on the other stereoisomers, due to the chiral C21 atom (Fig. 9) and the non-planar biphenyl skeleton, lead to the same results.

## Conclusion

A study by mass spectrometry and thermal (TG and DSC) techniques of a phenolic dibenzodioxocin lignin model, 4-(4,9-dimethoxy-2,11-*n*-dipropyl-6,7-dihydro-5,8-dioxa-dibenzo[a,c]cycloocten-6-yl)-2-methoxyphenol (DBDOH, **1**) shows that this compound is thermally unstable since at 150 °C giving vinylguaiacol (**2**) and 3,3′-dimethoxy-5,5′-dipropylbiphenyl-2,2′-diol (**3**) as decomposition products indicating that the two ether bonds of the dioxocin ring were broken. Quantum chemistry calculations show that the α–O-4 ether bond is expected to be broken first since its barrier energy for scission is lower than the *β*–O-4 ether one by roughly 50 kJ $mol^{-1}$. This conclusion is likely applicable to thermal degradation of DBDO units in lignin polymer.

Another important conclusion of this theoretical study is the following: similarity of semi-empirical and DFT results demonstrates clearly that, if a correct description of the non-dynamical correlation is taken into account, use of the AM1 parameterization is as justified as DFT to compare these two bond dissociation channels.

**Acknowledgments** RR and AC acknowledge Leandro Gustavo da Silva (Laboratorio de Fotoquímica e Materiais Lignocelulósicos, Universidade Federal de Uberlândia,, Brazil) for his help in thermal measurements (TG and DSC).

## References

Akim LG, Colodette JL, Argyropoulos DS (2001) Factors limiting oxygen delignification of kraft pulp. Can J Chem 79:201–210

AMPAC$^{TM}$ 9 (1992–2008) Semichem, Inc. 12456 W 62nd Terrace—Suite D Shawnee, KS 66216. http://www.semichem.com/ampacmanual/index.html. Accessed 6 March 2011

Argyropoulos DS (2003) Salient reactions in lignin during pulping and oxygen bleaching: an overview. J Pulp Pap Sci 29:308–313

Argyropoulos DS, Jurasek L, Kristofova L, Xia Z, Sun Y, Palus E (2002) Abundance and reactivity of dibenzodioxocins in softwood lignin. J Agric Food Chem 50:658–666

Becke AD (1993) A new mixing of Hartree-Fock and local density-functional theories. J Chem Phys 98:1372–1377

Black M, Cadogan JIG, McNab H (1994) Pyrolysis of O-allyl salicylic amides and esters, and related compounds: Formation of isoindolones and phthalides. J Chem Soc Perkin Trans I:155–159

Domburg GE, Sergeeva VN, Zheibe GA (1970) Thermal analysis of some lignin model compounds. J Thermal Anal 2:419–429

Dougherty RC (1974) The relationship between mass spectrometric, thermolytic and photolytic reactivity. Top Curr Chem 45:93–138

Elder T (2010) A computational study of pyrolysis reactions of lignin model compounds. Holzforschung 64:435–440

Gardrat C, Ruggiero R, Hoareau W, Nourmamode A, Grelier S, Siegmund B, Castellan A (2004) Photochemical study of an O-ethyl dibenzodioxocin molecule as a model for the photodegradation of non-phenolic lignin units of lignocellulosics. J Photochem Photobiol A Chem 167:111–120

Gardrat C, Ruggiero R, Hoareau W, Damigo L, Nourmamode A, Grelier S, Castellan A (2005) Photochemical study of 4-(4,9-dimethoxy-2,11-n-dipropyl-6,7-dihydro-5,8-dioxa-dibenzo[a, c]cyc-loocten-6-yl)-2-methoxyphenol, a lignin model of phenolic dibenzodioxocin unit. J Photochem Photobiol A Chem 169:259–267

Gaussian 09, Revision **A.1** (2009) Frisch MJ, Trucks GW, Schlegel HB, Scuseria GE, Robb MA, Cheeseman JR, Scalmani G, Barone V, Mennucci B, Petersson GA, Nakatsuji H, Caricato M, Li X, Hratchian HP, Izmaylov AF, Bloino J, Zheng G, Sonnenberg JL, Hada M, Ehara M, Toyota K, Fukuda R, Hasegawa J, Ishida M, Nakajima T, Honda Y, Kitao O, Nakai H, Vreven T, Montgomery Jr JA, Peralta JE, Ogliaro F, Bearpark M, Heyd JJ, Brothers E, Kudin KN, Staroverov VN, Kobayashi R, Normand J, Raghavachari K, Rendell A, Burant JC, Iyengar SS, Tomasi J, Cossi M, Rega N, Millam NJ, Klene M, Knox JE, Cross JB, Bakken V, Adamo C, Jaramillo J, Gomperts R, Stratmann RE, Yazyev O, Austin AJ, Cammi R, Pomelli C, Ochterski JW, Martin RL, Morokuma K, Zakrzewski VG, Voth GA, Salvador P, Dannenberg JJ, Dapprich S, Daniels AD, Farkas Ö, Foresman JB, Ortiz JV, Cioslowski J, Fox DJ; Gaussian, Inc., Wallingford CT. www.gaussian.com/g_tech/g_ur/m_citation.htm. Accessed 26 Mar 2012

Karhunen P, Rummako P, Sipilä J, Brunow G (1995a) Dibenzodioxocins; a novel type of linkage in softwood lignins. Tetrahedron Lett 36:169–170

Karhunen P, Rummako P, Sipilä J, Brunow G, Kilpeläinen I (1995b) The formation of dibenzodioxocin structures by oxidative coupling. A model reaction for lignin biosynthesis. Tetrahedron Lett 36:4501–4504

Karhunen P, Rummako P, Pajunen A, Brunow G (1996) Synthesis and crystal structure determination of model compounds for the dibenzodioxocine structure occurring in wood lignins. Chem Soc Perkin Trans 1:2303–2308

Karhunen P, Mikkola J, Pajunen A, Brunow G (1999) The behaviour of dibenzodioxocin structures in lignin during alkaline pulping processes. Nordic Pulp Paper Res 14:123–129

Kawamoto H, Horigoshi S, Saka S (2007) Pyrolysis reactions of various lignin model dimers. J Wood Sci 53:168–174

Kishimoto T, Sano Y (2003) Delignification mechanism during high-boiling solvent pulping. 4. Effect of a reducing sugar on the degradation of guaiacylglycerol-beta-guaiacyl ethers. J Wood Chem Technol 23:233–248

Kishimoto T, Ueki A, Takamori H, Uraki Y, Ubukata M (2004) Delignification mechanism during high boiling solvent pulping. 6. Change in lignin structure analyzed by $^{1}H$–$^{13}C$ correlation 2D NMR spectroscopy. Holzforschung 58:355–362

Kudanga T, Prasetyo EN, Sipila J, Nyanhongo GS, Guebitz GM (2010) Enzymatic grafting of functional molecules to the lignin model dibenzodioxocin and lignocellulosic material. Enzyme Microbiol Technol 46:272–280

Kukkola EM, Koutaniemi S, Gustafsson M, Karhunen P, Ruel K, Lundell TK, Saranpa P, Brunow G, Teeri TH, Fagerstedt KV (2003) Localization of dibenzodioxocin substructures in lignifying Norway spruce xylem by transmission electron microscopy-immunogold labelling. Planta 217:229–237

Machado AEH, De Paula R, Ruggiero R, Gardrat C, Castellan A (2006) Photophysics of dibenzodioxocins. J Photochem Photobiol A Chem 180:165–174

Mc Lafferty FW, Turecek F (1993) Interpretation of mass spectra, 4th edn. University Science Books, Mill Valley CA

Nakamura T, Kawamoto H, Saka S (2008) Pyrolysis behavior of Japanese cedar wood lignin studied with various model dimers. J Anal Appl Pyrolysis 81:173–182

Schummer C, Delhomme O, Appenzeller BMR, Wennig R, Millet M (2009) Comparison of MTBSTFA and BSTFA in derivatization reactions of polar compounds prior to GC/MS analysis. Talanta 77:1473–1482

Zawisza A, Toupet L, Sinou D (2006) A concise approach to the dibenzo[1,4]dioxocin structure. Lett Org Chem 3:861–864

Zhao P, Truhlar DG (2008) Density functionals with broad applicability in chemistry. Accounts Chem Res 41:157–167